COUPLING PLASTICITY AND ENERGY-CONSERVING ELASTICITY MODELS FOR CLAYS

By Ronaldo I. Borja,[1] Claudio Tamagnini,[2] and Angelo Amorosi[3]

ABSTRACT: A class of two-invariant stored energy functions describing the hyperelastic characteristics of soils is coupled with a critical-state plasticity model. The functions include constant as well as pressure-dependent elastic shear modulus models, and automatically satisfy the requirement that the elastic response for any loading path be energy conserving. The elastic responses predicted by the hyperelastic model are compared with measured undrained elastic responses of an overconsolidated clay in order to assess, both qualitatively and quantitatively, the predictive capability of the hyperelastic model. The importance of the pressure-dependent nature of the elastic shear modulus is assessed within the context of elastic and plastic responses. An energy-conserving model provides a fundamentally correct description of elastic material behavior even in the regime of plastic responses.

INTRODUCTION

Nonlinear elasticity is a critical component of elastoplastic constitutive models for soils. In the past, linear elasticity and isotropy were often considered as sufficient assumptions for capturing the elastic behavior of most metals with reasonable accuracy. However, the inappropriateness of these assumptions for granular materials such as soils, particularly that of linear elasticity, is now generally well recognized. Many constitutive models developed for soils are now in fact capable of handling the case of nonlinear elasticity (Wroth 1972; Vermeer 1978; Boyce 1980; Mroz and Norris 1982; Houlsby 1985; Wroth and Houlsby 1985; Loret 1985; Jardine et al. 1986; Ortiz and Simo 1986; Lade and Nelson 1987; Britto and Gunn 1987; Gens and Potts 1988; Molenkamp 1988; Borja and Lee 1990; Borja 1991; Hueckel et al. 1992; Simo and Meschke 1993).

Elasticity models are commonly incorporated into elastoplastic constitutive models through a hypoelastic formulation. This approach may be traced historically from parallel developments in the theory of plasticity employing rate-type constitutive equations (Hill 1967; Kachanov 1971). However, extension of a hypoelastic formulation to the case of nonlinear elastic soil response could result, in some cases, in nonconservative models. For example, the formulation of Simpson (1973), in which the elastic bulk and shear moduli are linear functions of the effective confining stress and related through a constant Poisson's ratio, leads to a model that does not conserve energy (Zytynski et al. 1978). On the other hand, hyperelastic materials are those for which a stored energy function exists, and hence, are conservative. The stored energy function for linear elasticity is clearly given by a quadratic functional, but for nonlinear elasticity the form of the stored energy function is not as obvious.

Energy-conserving elasticity models for sands have been presented by Vermeer (1978), Boyce (1980), Loret (1985), Lade and Nelson (1987), and Molenkamp (1988), among others. The issue deals with incorporating the observed strong dependence of the elastic bulk and shear moduli on the effective confining stress within the framework of a conservative elasticity model. Restricting to the case of isotropy, models having this feature require that the elastic bulk and shear moduli be functions of both the first and second stress invariants, but not of the third stress invariant. Equivalently, some form of elastic coupling of the volumetric and deviatoric responses must be provided or the model will incorrectly generate/dissipate energy over a closed elastic stress path.

A few investigators have provided some useful insight into the elastic behavior of overconsolidated clays. Again, restricting the discussion to the case of isotropy, Wroth (1972), and Wroth and Houlsby (1985) proposed an elasticity model for overconsolidated clays in which the bulk and shear moduli are normalized with respect to the mean effective normal stress through an expression that varies with the logarithm of the overconsolidation ratio. Rampello et al. (1994, 1995) provided an exponential approximation for the shear modulus from results of bender element tests, which predicts a similar trend. As for Wroth's (1972) model, which was developed primarily from the 1967 experimental results of Webb for London clay, it is, strictly speaking, not conservative because of its use of a constant Poisson's ratio. Hueckel et al. (1992) attempted to derive a hyperelastic model out of Wroth's model by introducing some form of elastoplastic coupling, but this new model had an undesirable feature—the elastic response is a function of the plastic response, and vice versa. Ignoring the effect of overconsolidation ratio, Houlsby (1985) proposed an expression for free energy function for clays that results in coupled elastic volumetric and deviatoric responses similar to the form presented by Mroz and Norris (1982). Houlsby's model is conservative, and takes into account the dependence of the elastic bulk and shear moduli on the effective confining stress.

Plasticity models for clays are far better developed than their nonlinear elasticity counterparts. It is not the objective of this paper to focus on such plasticity models—we simply refer the readers to, among others, Gens and Potts (1988) for a survey of existing plasticity models for soils, and Duncan (1996) for a survey of existing computer codes utilizing these models. Not surprisingly, very few energy-conserving nonlinear elasticity models for soils have found their way into multipurpose elastoplastic finite element (FE) codes. To the knowledge of the writers, the only such model that has been successfully implemented in practice is the isotropic elasticity model with pressure-dependent bulk modulus and constant shear modulus (Ortiz and Simo 1986; Britto and Gunn 1987; Simo and Meschke 1993). Coupling a plasticity model with a nonlinear elasticity model is not trivial, and the numerical implementation of the coupled model can indeed by very complex. Within the context of large-scale FE analysis, the complexity is exacerbated by the fact that the overall performance

[1]Assoc. Prof., Dept. of Civ. Engrg., Stanford Univ., Stanford, CA 94305-4020.

[2]Postdoctoral Scholar, Dept. of Civ. Engrg., Stanford Univ., Stanford, CA.

[3]Postdoctoral Res., Dept. of Struct. and Geotech. Engrg., Università Degli Studi di Roma "La Sapienza," Rome, Italy.

Note. Discussion open until March 1, 1998. To extend the closing date one month, a written request must be filed with the ASCE Manager of Journals. The manuscript for this paper was submitted for review and possible publication on May 13, 1996. This paper is part of the ***Journal of Geotechnical and Geoenvironmental Engineering***, Vol. 123, No. 10, October, 1997. ©ASCE, ISSN 1090-0241/97/0010-0948–0957/$4.00 + $.50 per page. Paper No. 11150.

of the constitutive model is not tested on the Gauss point level, but on the mesh level, where important structural details and boundary conditions can influence the overall response (Hughes 1984).

The objective of this paper is to present a systematic approach for coupling conventional plasticity models for clays with a nonlinear elasticity model with pressure-dependent bulk and shear moduli. To this end, we generalize the hyperelastic function of Houlsby (1985) to include the constant as well as the variable elastic shear moduli cases, and combine the resulting model with the modified Cam-clay plasticity model of Roscoe and Burland (1968). The approach does not involve elastoplastic coupling in the sense of Hueckel et al. (1992), since the elasticity and plasticity models remain completely intact in the present formulation. Thus, the proposed approach may be applied equally well to any similar plasticity model such as those advocated by the Cambridge group (Schofield and Wroth 1968). However, a notable modification to the plasticity theory used in the present formulation lies in the use of a bilogarithmic compressibility law, proposed independently by Hashiguchi and Ueno (1977) and Butterfield (1979), to describe the hardening response of the soil. As demonstrated by these investigators, the bilogarithmic compressibility law improves the predictive capability of the plasticity model in many cases. Furthermore, Borja and Tamagnini (in press, 1997) demonstrated that this hardening law can also be used in the regime of finite strains, as well as lead to an analytical expression that is far simpler to implement than the conventional linear void ratio-logarithm of effective stress model.

NONLINEAR ELASTICITY MODEL

The conventional solution of incremental plasticity problems is based on the integration of the rate-constitutive equation

$$\dot{\sigma}_{ij} = c^e_{ijkl}\dot{\varepsilon}^e_{kl}; \quad \dot{\varepsilon}^e_{kl} = \dot{\varepsilon}_{kl} - \dot{\varepsilon}^p_{kl} \tag{1a,b}$$

where σ_{ij} = effective Cauchy stress tensor; ε_{kl} = small strain tensor; c^e_{ijkl} = elastic stress-strain tensor; superscripts e and p = elastic and plastic components, respectively; and the overdots imply a time differentiation. By assuming isotropy and linear elasticity, the elastic stress-strain tensor c^e_{ijkl} can be expressed in terms of the elastic bulk modulus K and elastic shear modulus μ.

For soils the dependence of the elastic moduli K and μ on the effective confining stress is generally well recognized. To incorporate this important feature, the rate-constitutive equation (1) is usually reformulated in terms of the variable elastic moduli (Simpson 1973; Atkinson 1980; Britto and Gunn 1987; Gens and Potts 1988; Borja and Lee 1990)

$$K = \left(\frac{1 + e}{\kappa}\right) p; \quad \mu = \frac{3K(1 - 2\nu)}{2(1 + \nu)} \tag{2a,b}$$

where p = mean normal stress; e = void ratio; κ = swell-recompression index; and ν = constant elastic Poisson's ratio. The first of (2) assumes that the volumetric unload-reload curve involves a purely elastic process, and that the hysteretic behavior exhibited by soils during unloading and reloading is small. Although the elasticity model described here is widely used, it is known to be nonconservative (Zytynski et al. 1978).

Hyperelastic Model

The formulation of hyperelasticity is based on the existence of a stored energy function $\psi = \psi(\varepsilon^e_{ij})$, where ε^e_{ij} = elastic component of the small strain tensor. The effective Cauchy stress tensor σ_{ij} can be expressed in terms of ψ as

$$\sigma_{ij} = \frac{\partial \psi}{\partial \varepsilon^e_{ij}} \tag{3}$$

Furthermore, the elastic moduli tensor can be expressed as

$$c^e_{ijkl} = \frac{\partial \sigma_{ij}}{\partial \varepsilon^e_{kl}} = \frac{\partial^2 \psi}{\partial \varepsilon^e_{ij} \partial \varepsilon^e_{kl}} \tag{4}$$

The major symmetry of c^e_{ijkl} follows immediately from the assumption that the function ψ does exist; the minor symmetry arises from the symmetry of the elastic component of the small strain tensor.

Now, consider a class of stored energy functions of the volumetric and deviatoric invariants of the small strain tensor, denoted by ε^e_v and ε^e_s, respectively. The invariants are defined as

$$\varepsilon^e_v = \varepsilon^e_{kk}; \quad \varepsilon^e_s = \sqrt{\frac{2}{3} e^e_{ij} e^e_{ij}}; \quad e^e_{ij} = \varepsilon^e_{ij} - \frac{1}{3}\varepsilon^e_v \delta_{ij} \tag{5a-c}$$

where δ_{ij} = Kronecker delta. Assuming a stored energy function of the form $\psi = \psi(\varepsilon^e_v, \varepsilon^e_s)$, then we can use the chain rule to expand (3) in the form

$$\sigma_{ij} = \frac{\partial \psi}{\partial \varepsilon^e_v}\frac{\partial \varepsilon^e_v}{\partial \varepsilon^e_{ij}} + \frac{\partial \psi}{\partial \varepsilon^e_s}\frac{\partial \varepsilon^e_s}{\partial \varepsilon^e_{ij}} \tag{6}$$

Setting

$$p = \frac{\partial \psi}{\partial \varepsilon^e_v}; \quad q = \frac{\partial \psi}{\partial \varepsilon^e_s} \tag{7a,b}$$

then (6) takes the form

$$\sigma_{ij} = p\delta_{ij} + \sqrt{\frac{2}{3}}\, q \hat{n}_{ij} \tag{8}$$

where $\hat{n}_{ij} = \sqrt{2/3} e^e_{ij}/\varepsilon^e_s$. One can easily recognize that p and q are, respectively, the mean normal stress and the deviatoric invariant of the effective Cauchy stress tensor, and are given explicitly by the expressions

$$p = \frac{1}{3}\sigma_{kk}; \quad q = \sqrt{\frac{3}{2} s_{ij} s_{ij}}; \quad s_{ij} = \sigma_{ij} - p\delta_{ij} \tag{9a-c}$$

The elastic moduli tensor can be obtained by differentiating the stress equation (7) with respect to the corresponding strain components. In so doing, the following 2×2 Hessian matrix of ψ will be required (Borja and Tamagnini, in press, 1997)

$$\mathbf{D}^e = \begin{bmatrix} D^e_{11} & D^e_{12} \\ D^e_{21} & D^e_{22} \end{bmatrix} = \begin{bmatrix} \partial^2\psi/\partial\varepsilon^e_v\partial\varepsilon^e_v & \partial^2\psi/\partial\varepsilon^e_v\partial\varepsilon^e_s \\ \partial^2\psi/\partial\varepsilon^e_s\partial\varepsilon^e_v & \partial^2\psi/\partial\varepsilon^e_s\partial\varepsilon^e_s \end{bmatrix} \tag{10}$$

The matrix $\mathbf{D}^e$ has the physical significance of being the tangential invariant stress-invariant elastic strain matrix, and satisfies the rate equation

$$\begin{Bmatrix} \dot{p} \\ \dot{q} \end{Bmatrix} = \begin{bmatrix} D^e_{11} & D^e_{12} \\ D^e_{21} & D^e_{22} \end{bmatrix} \begin{Bmatrix} \dot{\varepsilon}^e_v \\ \dot{\varepsilon}^e_s \end{Bmatrix} \tag{11}$$

Note that $\mathbf{D}^e$ is symmetric provided that the function ψ exists. If $D^e_{12} \neq 0$, then the volumetric and deviatoric elastic responses couple, that is, an imposed volumetric strain produces a shearing stress response, and vice versa. The following section investigates the significance of these coupled elastic responses within the context of a stored energy function developed specifically for cohesive soils.

Stored Energy Function

Consider a class of stored energy functions of the form

$$\psi(\varepsilon^e_v, \varepsilon^e_s) = p_0\tilde{\kappa} \exp\left(\frac{\varepsilon^e_v - \varepsilon^e_{v0}}{\tilde{\kappa}}\right) + \frac{3}{2}\mu\varepsilon^{e2}_s \tag{12}$$

where ε^e_{v0} = elastic volumetric strain corresponding to a mean normal stress of p_0; $\tilde{\kappa}$ = elastic compressibility index; and $\mu = \mu(\varepsilon^e_v)$ = elastic shear modulus defined by the expression

$$\mu = \mu_0 + \alpha p_0 \exp\left(\frac{\varepsilon^e_v - \varepsilon^e_{v0}}{\tilde{\kappa}}\right) \tag{13}$$

The elastic shear modulus μ contains a constant term μ_0 and a term that varies with the elastic volumetric strain through the constant coefficient α. If $\alpha = 0$ and $\mu_0 > 0$, then the elasticity model is defined by a variable elastic bulk modulus and a constant elastic shear modulus; if $\alpha > 0$ and $\mu_0 = 0$, then the stored energy function (12) reduces to the model presented by Houlsby (1985). Although μ_0 and α can both take on nonzero values, we will restrict this paper to the two previously described extreme cases where only one of these two parameters is nonzero.

The following elastic constitutive equations can be derived from (12):

$$p = p_0\beta \exp\left(\frac{\varepsilon^e_v - \varepsilon^e_{v0}}{\tilde{\kappa}}\right); \quad q = 3\mu\varepsilon^e_s \tag{14a,b}$$

where $\beta = 1 + 3\alpha(\varepsilon^e_s)^2/2\tilde{\kappa}$. Differentiating p with respect to ε^e_v gives the tangential elastic bulk modulus

$$D^e_{11} \equiv K = \frac{p}{\tilde{\kappa}} = \frac{p_0}{\tilde{\kappa}}\beta \exp\left(\frac{\varepsilon^e_v - \varepsilon^e_{v0}}{\tilde{\kappa}}\right) \tag{15}$$

Thus, we recover an important feature of elastic soil behavior that the elastic bulk modulus K be a linear function of p. The elastic shear modulus is given by

$$D^e_{22}/3 \equiv \mu = \mu_0 + \left(\frac{\alpha}{\beta}\right)p = \mu_0 + \alpha p_0 \exp\left(\frac{\varepsilon^e_v - \varepsilon^e_{v0}}{\tilde{\kappa}}\right) \tag{16}$$

Thus, with a suitable choice of parameters, μ can be made either constant or a linear function of p. The coupling terms D^e_{12} and D^e_{21} in (10) are given by

$$D^e_{12} = D^e_{21} = \left(\frac{3\alpha\varepsilon^e_s}{\beta\tilde{\kappa}}\right)p = \frac{3\alpha p_0\varepsilon^e_s}{\tilde{\kappa}} \exp\left(\frac{\varepsilon^e_v - \varepsilon^e_{v0}}{\tilde{\kappa}}\right) \tag{17}$$

Since the coupling terms can be nonzero for $\alpha \neq 0$, the elastic shear and volumetric responses are coupled for a general loading path. Furthermore, if $\mu_0 = 0$ and $\varepsilon^e_s = \sqrt{2\tilde{\kappa}/3\alpha}$, then $\det(\mathbf{D}^e) = 0$, and so the Hessian matrix of ψ becomes singular. This situation arises when the stress ratio q/p reaches its maximum attainable value of $\sqrt{3\alpha\tilde{\kappa}/2}$ (Houlsby 1985).

One way of investigating if the constant or the variable elastic shear modulus model should be used for a given soil is to perform undrained triaxial loading tests on overconsolidated soil samples starting at different values of the stress ratio q/p, and then plotting the resulting stress paths on the p-q plane. Since for these soils $d\varepsilon^e_v = 0$ during undrained loading, then

$$\frac{dp}{dq} = \frac{D^e_{12}}{D^e_{22}} = \left(\frac{3\alpha\varepsilon^e_s}{\beta\tilde{\kappa}}\right)\frac{p}{3\mu} \tag{18}$$

Now, if $\mu_0 = 0$ and $\alpha > 0$, then

$$\frac{dp}{dq} = \frac{\varepsilon^e_s}{\tilde{\kappa}} = \left[\frac{1}{3\alpha\tilde{\kappa}} + \frac{1}{2}\left(\frac{dp}{dq}\right)^2\right]\frac{q}{p} \tag{19}$$

which implies that the slope dp/dq varies nonlinearly with the stress ratio q/p as an effect of the volumetric-deviatoric coupling of the elastic response. On the other hand, if $\alpha = 0$ and $\mu_0 > 0$, then $dp/dq = 0$, which implies that during undrained loading the stress path is perpendicular to the volumetric axis p. The actual slope dp/dq exhibited by the soil sample can then be used to assess which of the two models is more appropriate for this soil.

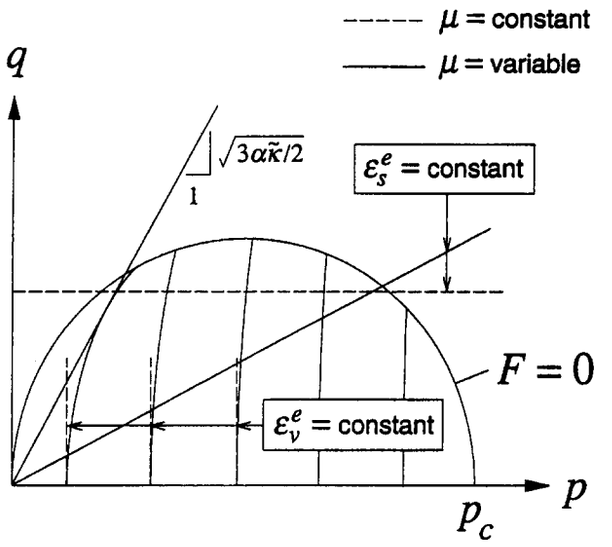

FIG. 1. Contours of Constant Elastic Volumetric and Deviatoric Strains for Hyperelastic Model

To further clarify the main points raised in the previous paragraph, consider the contours of constant ε^e_v and ε^e_s on the p-q plane for the proposed hyperelastic model shown in Fig. 1. This graphical representation was first presented by Houlsby (1985), and is reproduced here because of its relevance for interpreting the laboratory test results later reported in this paper. For the pressure-dependent shear modulus model, the undrained stress paths in the overconsolidated region are identical to contours of constant ε^e_v, and are given by a family of curves shown in Fig. 1. The maximum attainable stress ratio $(q/p)_{max} = \sqrt{3\alpha\tilde{\kappa}/2}$ may be interpreted as a straight line through the origin to which all undrained stress paths eventually become tangent [because of its high value, this maximum stress ratio is unlikely to be attained by real soils (Houlsby 1985)]. Contours of constant ε^e_s are represented by constant stress ratio lines, since (15) and (17) yield $q/p = 3\alpha\varepsilon^e_s/\beta$ = constant. On the other hand, for the constant shear modulus model the undrained stress paths in the overconsolidated region are defined by a family of vertical lines, since $\dot{\varepsilon}^e_v = 0$ implies $\dot{p} = 0$ due to the uncoupled volumetric and deviatoric responses. Finally, a trivial result, q = constant, characterizes the condition ε^e_s = constant for the constant elastic shear modulus model.

The choice of the stored energy function (12) offers the advantage that it takes into account the dependence of the elastic bulk and shear moduli on the effective confining stress, in addition to assuring a conservative elastic model. It is also convenient to use because it is defined in the space of elastic strains. As shown in the following section, elastic strains are used as primary state variables in the integration algorithm, and so this feature can be exploited to integrate the constitutive equation accurately. However, the resulting constitutive model predicts an elastic shear modulus that varies linearly with the mean normal stress, which may not be a very accurate description of observed clay shear behavior (Wroth and Houlsby 1985; Rampello et al. 1994, 1995). Nevertheless, this elasticity model offers a good compromise between accuracy, fundamental correctness, and ease of implementation, and is thus used here in conjunction with the plasticity model that follows.

PLASTICITY MODEL

The essential ingredients of a plasticity model are a yield function, a flow rule, and a hardening law. As a matter of illustration, let us assume a two-invariant yield function of the form

$$F = F(p, q, p_c) = 0 \tag{20}$$

where p and q = invariants defined in (7), and p_c = scalar plastic state variable describing the size of the yield function F. The ellipsoid of modified Cam-clay theory (Roscoe and Burland 1968) is an example of a yield surface that can be put in the aforementioned form, with p_c having the physical significance of being the preconsolidation pressure.

On invoking the associative flow rule, the plastic strain rate $\dot{\varepsilon}_{ij}^p$ can be evaluated from the yield function F as

$$\dot{\varepsilon}_{ij}^p = \dot{\Lambda} \frac{\partial F}{\partial \sigma_{ij}} \tag{21}$$

where $\dot{\Lambda} \geq 0$ is a parameter obtained from imposing the plastic consistency condition. Bounding surface formulation also provides a similar expression for $\dot{\varepsilon}_{ij}^p$, except that F is now replaced by some suitably defined plastic potential function, and $\dot{\Lambda} \geq 0$ is obtained from some plastic hardening modulus that depends on the location of the stress point with respect to the image point [see Eq. (10.5) of Dafalias and Herrmann (1982) for the case of associative plasticity].

Bilogarithmic Compressibility Law

The growth of p_c is conventionally defined by a linear relationship between the void ratio e and the logarithm of p_c, or, equivalently, by a linear variation of the specific volume $v = (1 + e)$ with the logarithm of p_c. The limitations of this hardening law are generally well recognized and include, among others, that a negative void ratio can result even at realistically low values of the preconsolidation pressure, and that the linear relationship is valid only over a narrow range of values of the effective volumetric stress.

An alternative hardening law, which appears to have been first proposed by Hashiguchi and Ueno (1977), and later studied more extensively by Butterfield (1979) and Hashiguchi (1995), is of the form

$$\frac{\dot{v}}{v} = -\tilde{\lambda} \frac{\dot{p}_c}{p_c} \tag{22}$$

where $\tilde{\lambda}$ = compressibility soil index for virgin loading. A simple integration of (22) yields the relationship

$$\ln\left(\frac{v}{v_0}\right) = -\tilde{\lambda} \ln\left(\frac{p_c}{p_{c0}}\right) \tag{23}$$

which indicates a linear variation of $\ln v$ with $\ln p_c$. Eq. (23) can also be written in the form

$$\frac{v}{v_0} = \left(\frac{p_{c0}}{p_c}\right)^{\tilde{\lambda}} \tag{24}$$

which implies that v approaches zero as p_c approaches infinity. Since v cannot in principle have a value less than unity, then the bilogarithmic compressibility law (23) is not without a limitation either. However, Butterfield (1979) shows from compression test data on natural soils, specifically soft clays, that this law is more accurate than the unilogarithmic compressibility equation over a wider range of values of the effective volumetric stress. Furthermore, the value of p_c below which $e > 0$ (and hence, $v > 1$) is higher with the bilogarithmic compressibility law. In light of these desirable features, we shall use the bilogarithmic law (23) in the mathematical model that follows.

A simple inspection of (23) shows that in the limit of small strains, the natural volumetric strain $\ln(v/v_0) = \ln(1 - \Delta v/v_0)$, where $\Delta v = v_0 - v$, coincides with the nominal volumetric strain $\Delta v/v_0$ of the infinitesimal theory. Thus, the bilogarithmic hardening law approaches the unilogarithmic law in the limit of small volumetric strains. However, large deformation analysis requires the use of natural, and not nominal, strains (Borja and Alarcón 1995), and so (23) is analytically more robust since it is useful both for small and finite deformation analyses. The next section shows that the hardening law given by (23) offers a further computational advantage in that the evolution equation for p_c can now be integrated exactly over a finite load increment.

Stress Integration Algorithm

As mentioned in the introduction, the true test of the utility of a constitutive model lies in its efficient implementation. Hence, the algorithm for stress-point integration must be robust enough to accommodate the strongly nonlinear response predicted by the constitutive model. In this section, we present a novel stress-point integration algorithm carried out in the strain invariant space that applies to any two-invariant hyperelastic-plastic models of the form described in the previous section.

Assume that the total strain tensor can be decomposed additively into an elastic part and a plastic part. Using the backward implicit scheme, the integrated flow rule at time t_{n+1} takes the form

$$\varepsilon_{ij}^e|_{n+1} = \varepsilon_{ij}^{e,tr}|_{n+1} - \Lambda \frac{\partial F}{\partial \sigma_{ij}}|_{n+1} \tag{25}$$

where $\varepsilon_{ij}^{e,tr}|_{n+1} = \varepsilon_{ij}^e|_n + \Delta\varepsilon_{ij}$; $\varepsilon_{ij}^e|_n$ = converged elastic strain tensor at time station t_n; $\Delta\varepsilon_{ij}$ = imposed incremental strain tensor; and $\Lambda \geq 0$ is a consistency parameter. From a computational standpoint, (25) now requires that the elements of the tensor $\varepsilon_{ij}^e|_{n+1}$ be stored in the computer memory. The elements of the stress tensor σ_{ij} can then be derived uniquely through the free energy function ψ (Borja and Tamagnini 1995).

Omitting the subscripts $(n + 1)$ for brevity, the integrated flow rule in the strain invariant space takes the form

$$\varepsilon_v^e = \varepsilon_v^{e,tr} - \Lambda \frac{\partial F}{\partial p} \tag{26}$$

and

$$\varepsilon_s^e = \varepsilon_s^{e,tr} - \Lambda \frac{\partial F}{\partial q} \tag{27}$$

where $\varepsilon_v^{e,tr} = \varepsilon_{kk}^{e,tr}$; $\varepsilon_s^{e,tr} = \sqrt{2e_{ij}^{e,tr}e_{ij}^{e,tr}/3}$; and $e_{ij}^{e,tr} = \varepsilon_{ij}^{e,tr} - \varepsilon_v^{e,tr}\delta_{ij}/3$. With the algorithm driven by the total strain tensor $\varepsilon_{ij}^{e,tr}$, (26) and (27) describe the evolutions of the first and second elastic strain invariants, respectively. The consistency condition is imposed by the yield function (20), now written in terms of the elastic strain invariants as

$$F[p(\varepsilon_v^e, \varepsilon_s^e), q(\varepsilon_v^e, \varepsilon_s^e), p_c] = 0 \tag{28}$$

The evolution of p_c can be developed from the bilogarithmic compressibility (22). Here, we note that $\dot{\varepsilon}_v = -\dot{v}/v$ represents the volumetric strain rate, and takes the form

$$\dot{\varepsilon}_v = \tilde{\lambda} \frac{\dot{p}_c}{p_c} \tag{29}$$

On the other hand, the elastic component of the volumetric strain rate can be obtained from the hyperelastic constitutive (15). For purely isotropic loading, we have

$$\dot{\varepsilon}_v^e = \tilde{\kappa} \frac{\dot{p}}{p} = \tilde{\kappa} \frac{\dot{p}_c}{p_c} \tag{30}$$

since $p_c = p$ for soils yielding on the isotropic consolidation line. Subtracting (30) from (29) and rearranging gives

$$\frac{\dot{p}_c}{p_c} = \frac{1}{\tilde{\lambda} - \tilde{\kappa}} \dot{\varepsilon}_v^p \tag{31}$$

Assuming that (31) is valid for all possible stress paths involving plastic loading, then it can be integrated exactly as

$$p_c = p_{c,n} \exp\left(\frac{\varepsilon_v^p - \varepsilon_{v,n}^p}{\tilde{\lambda} - \tilde{\kappa}}\right) = p_{c,n} \exp\left(\frac{\varepsilon_v^{e,tr} - \varepsilon_v^e}{\tilde{\lambda} - \tilde{\kappa}}\right) \tag{32}$$

where $p_{c,n}$ = converged value of p_c at time station t_n. Note that this exact integration is not possible with the linear void ratio-logarithm of p_c relationship.

Turning now to (26) and (27), the derivatives of F can be obtained from (7) and (20) as

$$\frac{\partial F}{\partial p} = 2p - p_c = 2\frac{\partial \psi}{\partial \varepsilon_v^e} - p_c \tag{33}$$

and

$$\frac{\partial F}{\partial q} = \frac{2q}{M^2} = \frac{2}{M^2}\frac{\partial \psi}{\partial \varepsilon_s^e} \tag{34}$$

Eqs. (26)–(28) can be viewed as a system of three nonlinear equations in three unknowns, namely, ε_v^e, ε_s^e, and Λ. These equations can be solved quite easily by Newton-Raphson iterations (Borja and Tamagnini, in press, 1997). Once the unknowns have been determined, the elements of the effective stress tensor σ_{ij} can be evaluated from the hyperelastic constitutive (6).

The algorithm described previously has the computational advantage of being fully implicit, as opposed to the ones proposed by Borja and Lee (1990), Alawaji et al. (1992), and Hashash and Whittle (1992), among others, which involve explicit treatment of some internal variables. It has all the properties of the first-order backward implicit scheme, and is amenable to consistent linearization in closed form (Simo 1992).

TESTING PROGRAM AND NUMERICAL SIMULATIONS

For modeling purposes, we assume that the yield function F is given by the ellipsoid of modified Cam-clay theory (Roscoe and Burland 1968). The interior of the yield function is then characterized by a hyperelastic response. The first part of this section describes a laboratory testing program designed to assess the predictive capability of the model in the elastic regime. Here, experimental results for a stiff overconsolidated clay are compared with the model predictions to assess the performance of the hyperelastic model. In the second part, results of numerical simulations in the plastic range are compared with those obtained from a hypoelastic-plastic version of the model described by Borja and Lee (1990).

Testing Program and Validation

The soil under investigation is a stiff overconsolidated Plio-Pleistocene clay obtained from an adjacent site north of Rome, Italy, known locally as Vallericca clay (Amorosi 1996; Rampello et al. 1994). Block samples were obtained from a homogeneous in-situ deposit of this clay, from which triaxial specimens were made. Representative index properties of this clay are as follows. Specific gravity is $G_s = 2.78$, percent finer than 2 μm = 42%, liquid limit = 56.2%, plasticity index = 31.3%, natural water content = 26%, and calcium carbonate content = 30%. Oedometer tests indicate that the block samples had been subjected to an in-situ maximum vertical effective stress of about $\sigma_{v,c} \approx 2.60$ MPa.

Triaxial tests were carried out on five nearly identical 38.1-mm-diameter samples by means of a high pressure-controlled triaxial apparatus described by Amorosi (1996). Fig. 2 shows the imposed effective stress path on the p-q plane on these samples. For triaxial stress condition the stress invariants degenerate to the simple expressions $p = (\sigma_a + 2\sigma_r)/3$ and $q = |\sigma_a - \sigma_r|$; it is customary to assume $q = \sigma_a - \sigma_r$ for the deviatoric stress, without the absolute value symbols, and hence q can take on negative values ($q > 0$ for triaxial compression, $q < 0$ for extension).

Specimens were first anisotropically consolidated to an effective axial stress of $\sigma_{a,max} = 6.75$ MPa, which is about 2.6 times $\sigma_{v,c}$, along a path corresponding to a constant stress ratio of $q/p = 0.684$, or an equivalent lateral pressure coefficient of $K_0 = 0.53$, see Fig. 2. This value of K_0 was estimated from the formula proposed by Jaky (1944) for normally consolidated clays. Four of the five specimens were next unloaded to overconsolidation ratios of 1.7, 2.4, 3.8, and 8.9 corresponding to points D, C, B, and A, respectively, along the path shown in Fig. 2 (here, OCR = $\sigma_{a,max}/\sigma_{a,0}$, where $\sigma_{a,0}$ = final value of the effective axial stress on unloading but prior to undrained shearing). The unloading path corresponds to K_0 condition, in which K_0 was estimated from the formula proposed by Mayne and Kulhawy (1982) for overconsolidated clays. Undrained compressive shear tests were then carried out on all five samples under displacement control at a nominal axial strain rate of 5.6%/day. This relatively low value of the axial strain rate was chosen in order to obtain full equalization of the excess

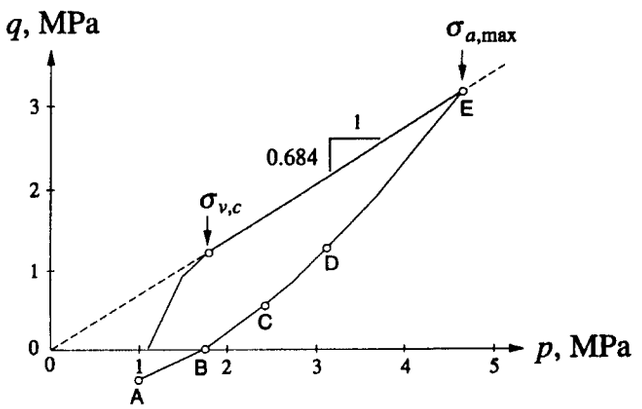

FIG. 2. Stress Path Prior to Undrained Shearing

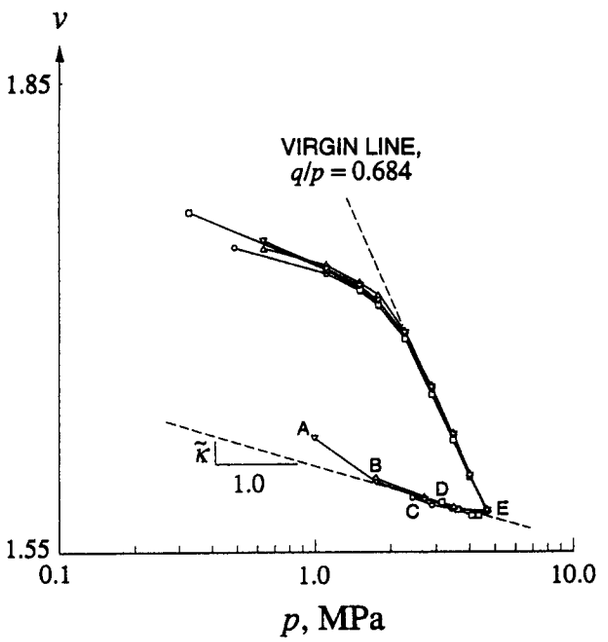

FIG. 3. Compression Curves on Log v-Log p Plane

pore pressure inside the specimen, and thus make the measured pore pressure values at the base of the sample meaningful.

Plots of the consolidation curves on the log v-log p plane for four triaxial samples are shown in Fig. 3. Note that the virgin curves are nearly straight, even in the high pressure range, thus affirming the validity of the bilogarithmic compressibility law. Although the unloading curves are not quite as straight as the virgin curves, an initial tangent to the unloading path can readily be constructed to provide an average value of the elastic compressibility parameter of $\tilde{\kappa} = 0.013$ for this clay.

The lack of straightness of the unloading curves shown in Fig. 3 may be attributed to many factors, including the accumulation of plastic deformation on reverse loading (Mroz and Norris 1982). In fact, even if the plastic deformation on reverse loading is small and the response is purely elastic, the unloading curves could still deviate from a straight line because of elastic coupling effects. To elaborate this point further, consider a loading condition where q/p = constant. With the variable elastic shear modulus model, Fig. 1 shows that this condition corresponds to ε_s^e = constant. By appeal to the first of (14), this condition also implies a linear plot of ln p versus ε_v^e. However, since the stress ratio q/p is not constant during the unloading stage, then the unloading curves of Fig. 3 are not straight, possibly because of shearing strain effects. The last statement underscores the fact that the notion of "elastic wall" as used in conventional Cam-clay models (Roscoe and Burland 1968) does not hold in the present model because of elastic coupling effects.

The four specimens have been unloaded at different values of stress ratio to see how the slope dp/dq at the beginning of the undrained shear stage is influenced by the stress ratio q/p. Fig. 4 shows the measured values of dp/dq as functions of the stress ratio q/p at the beginning of undrained stress paths for the four overconsolidated triaxial samples (the fifth sample is normally consolidated, and hence, cannot be used to validate the elastic model). The measured values of dp/dq were evaluated at initial compressive axial strains less than 0.1%; within the accuracy of the measurements performed, they can be considered representative of the slopes at the beginning of the undrained stress paths. Since the beginning of the undrained stress paths correspond to points of stress reversal, the initial slopes of these paths correspond to instantaneous elastic response. Observe that these measured initial slopes are never zero, except in the vicinity of the point corresponding to a stress ratio of $q/p = 0$. Furthermore, the slope is negative where q/p is negative, and is positive where q/p is positive (the sign changes according to the value of q). Similar results have been reported by Gens (1982) for Lower Cromer Till, a sandy clay of low plasticity similar to some soils encountered in the northern North Sea. This behavior indicates that this particular material shows significant volumetric-deviatoric elastic coupling. Moreover, the observed trend of the measurements is consistent with (19), indicating that the variable elastic shear modulus model is more appropriate for this soil than the constant elastic shear modulus model, since the latter would have predicted $dp/dq = 0$ for any value of the stress ratio. A least square fit using (19) of the theoretical function dp/dq on the measured slopes provides a value of the hyperelastic model parameter of $\alpha = 103$ (assuming $\mu_0 = 0$) for this soil.

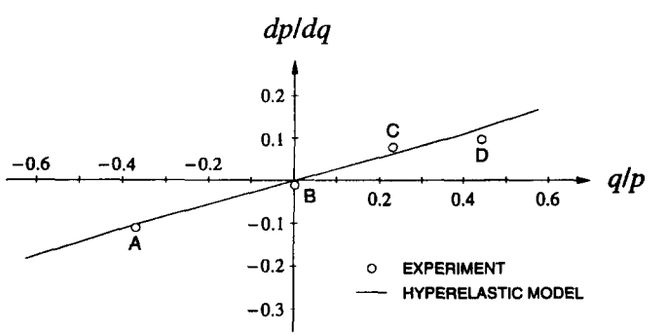

FIG. 4. Variation of dp/dq with Stress Ratio q/p ($\alpha = 103$, $\mu_0 = 0$)

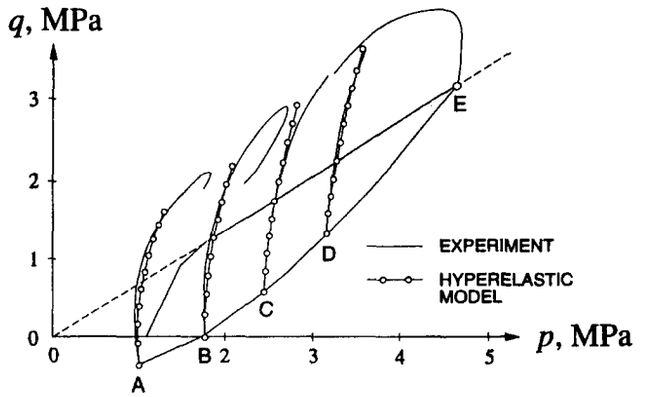

FIG. 5. Elastic Undrained Stress Paths on Vallericca Clay: Experiment versus Prediction

Fig. 5 shows a comparison between predicted and measured undrained stress paths. The agreement between model predictions and actual data is satisfactory provided that the stress point remains within the elastic region. Note that for $q/p < 0$ (point A), p decreases in magnitude during initial undrained loading, as manifested by an observed increase in pore water pressure during initial shearing. For the other two cases where $q/p > 0$ (points C and D), the slopes dp/dq exhibited by the undrained curves are positive. The case $q/p \approx 0$ (point B) showed an initial slope that is approximately vertical. At this point, the hyperelastic theory predicts an initial apparent value of Poisson's ratio of $\nu = (3 - 2\alpha\tilde{\kappa})/(6 + 2\alpha\tilde{\kappa}) = 0.04$ for the soil skeleton, but this is the only point on this particular undrained stress path where the material theoretically behaves in an isotropic elastic manner (Houlsby 1985).

As a point of clarification, one can always argue that clays also exhibit significant plastic deformation in the overconsolidated range. This is precisely the motivation for using bounding surface-type plasticity and other similar models in some cases (Dafalias and Herrmann 1982; Dafalias 1986). However, this is not pertinent to the present analysis when interpreting the slopes of the stress paths at the very beginning of the undrained loading process, as shown in Figs. 4 and 5. Any elastoplastic model, even those with a vanishing yield locus, should predict a purely elastic instantaneous response at the onset of reverse loading, or loading which involves significant stress path rotation [see Mroz and Norris (1982)]. Thus, the slopes plotted in Fig. 4 may be attributed in great part to elastic volumetric-deviatoric coupling. Whether or not plastic strains occur in the overconsolidated range does not invalidate this conclusion from a theoretical standpoint.

Comparison with Conventional MCC Model

This section compares the behavior predicted by the hyperelastic-plastic model with that predicted by the conventional modified Cam-clay model (Borja and Lee 1990). In a nutshell, the main features of the latter model, which make it different from the proposed model, are the following: (1) the elasticity model is based on a hypoelastic formulation in which the variable elastic moduli are given by Eq. (2); (2) the void ratio varies linearly with the logarithm of effective mean normal stress; and (3) the solution is advanced in time using a stress-

space return mapping algorithm. Note that the third feature only affects the numerical accuracy of the solution but has no implication on the physical material response (Borja and Lee 1990; Borja and Tamagnini 1995). Extensive accuracy analyses have been performed in the present study to ensure that the load steps used in the simulations are small enough for the solutions to be considered sufficiently exact for plotting purposes. Thus, any noted discrepancy in the predicted material responses will be attributed to differences in the analytical features of the constitutive models.

As a first example, we consider a cubical soil sample of unit dimensions and deforming in plane strain, see Fig. 6. The sample is assumed to be normally consolidated and subjected to an initial all-around confining stress of $p_0 = 90$ kPa. Three material types were considered for comparison: material type A is a hyperelastic-plastic material with a constant shear modulus, material type B is the same as material type A except that the elastic shear modulus varies with p, and material type C is a hypoelastic-plastic material with a constant Poisson's ratio. The parameters used for each material are summarized in Table 1. Note that the compression indices λ and κ of material type C are related to the compression indices $\tilde{\lambda}$ and $\tilde{\kappa}$ of material types A and B by the relations $\lambda = \tilde{\lambda} v_0$ and $\kappa = \tilde{\kappa} v_0$, where v_0 is the initial specific volume. The parameters shown in Table 1 have been selected so as to provide the same initial values of elastic shear moduli at the beginning of shearing. As for notations, n_0 = reference porosity; ν = Poisson's ratio; e_a = reference void ratio at unit preconsolidation pressure; and M = slope of the critical state line.

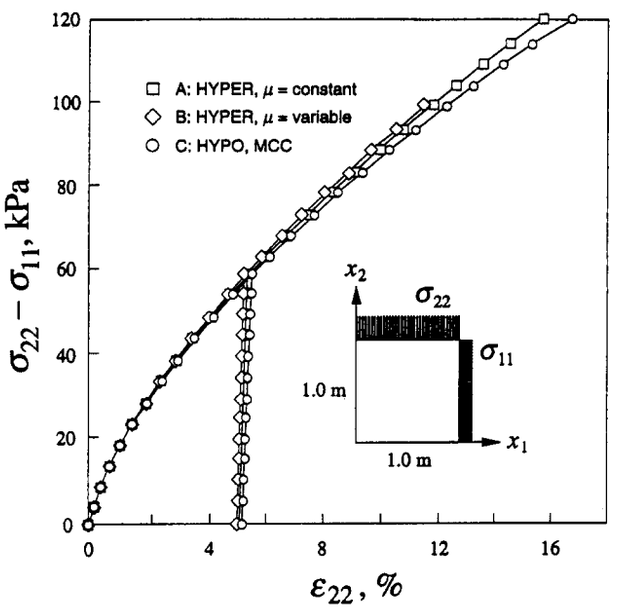

FIG. 6. Stress-Strain Curves for Plane Strain Example

TABLE 1. Material Parameters for Triaxial Test Simulations

Parameter (1)	Material Type A (2)	B (3)	C (4)
μ_0 (kPa)	5,400	0	0
α	0	60	0
ν	n/a	n/a	0.103
λ	n/a	n/a	0.433
κ	n/a	n/a	0.060
$\tilde{\lambda}$	0.130	0.130	n/a
$\tilde{\kappa}$	0.018	0.018	n/a
n_0	0.70	0.70	n/a
e_a	n/a	n/a	4.28
M	1.05	1.05	1.05

Fig. 6 shows a plot of the stress difference $\sigma_{22} - \sigma_{11}$ versus nominal axial strain ε_{22} as the soil is compressed vertically but allowed to move horizontally on the plane of shearing. Loading was done under a stress-controlled condition where σ_{22} was increased while σ_{11} was held fixed. At a stress difference of $\sigma_{22} - \sigma_{11} = 60$ kPa, the sample was unloaded to its initial isotropic state, and then reloaded back up again. As shown in Fig. 6, all three materials behaved nearly identically during the initial part of shearing. The slightly "softer" stress-strain response predicted by material type C is due primarily to the nature of the compressibility law used in this model.

Fig. 7 magnifies the unload-reload curves of Fig. 6. Note that the pressure-dependent nature of the elastic shear modulus used in material models B and C resulted in a gradual stiffening of the elastic response with increasing vertical stress. However, except for the slightly offset unloading curve for material type C, the unload/reload curves for all three materials are nearly the same.

As a second example, we consider triaxial soil samples described by the same material models A, B, and C as in the first example, and subjected to the same initial all-around confining stress of $p_0 = 90$ kPa. The specimens were then subjected to a closed stress path consisting of sequential isotropic and deviatoric loading and unloading as described in Table 2. Note that constant p-paths have been used in Table 2 instead of the standard triaxial compression paths where σ_r = constant so that the effect of pure deviatoric loading can be distinguished clearly from the effect of pure isotropic loading. A constant p-path under a triaxial stress condition entails increasing (or decreasing) the axial stress by an amount equal to twice the amount that the radial stress is decreased (or increased).

Fig. 8 shows the deviatoric stress q-deviatoric strain ε_s curves resulting from the imposed stress paths described

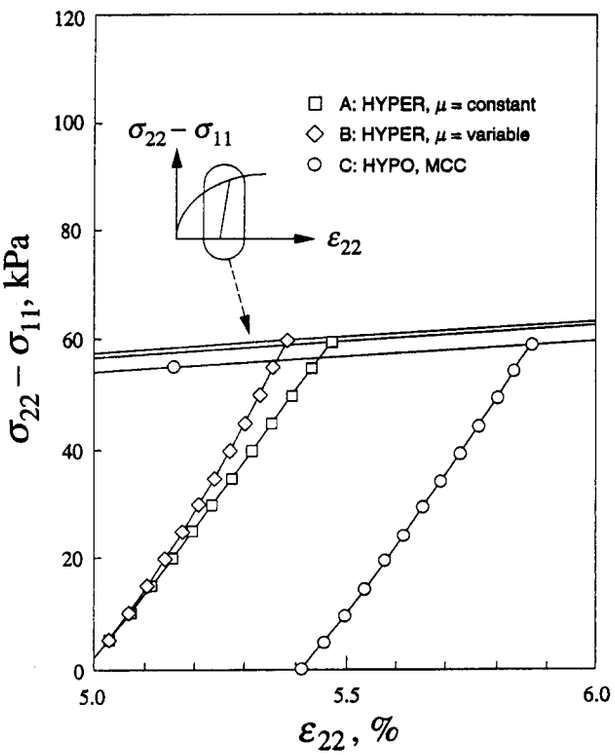

FIG. 7. Magnification of Unloading Curves for Plane Strain Example

TABLE 2. Stress Path for Triaxial Test Simulations

State number (1)	p (kPa) (2)	q (kPa) (3)	Description (4)
0	90.0	0.0	Initial condition
1	90.0	45.0	Deviatoric loading
2	180.0	45.0	Isotropic loading
3	180.0	90.0	Deviatoric loading
4	180.0	0.0	Deviatoric unloading
5	90.0	0.0	Isotropic unloading

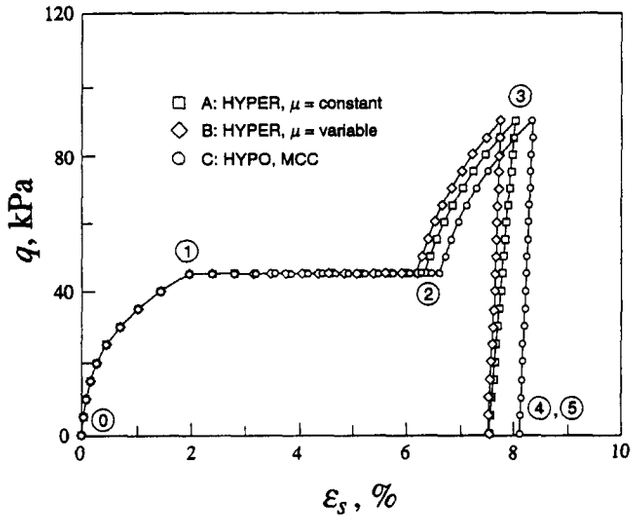

FIG. 8. Deviatoric Stress-Deviatoric Strain Curves for Closed Stress Path Triaxial Loading

in Table 2. Note that the predicted responses for all three materials are again nearly identical during the initial deviatoric loading since the elastic shear moduli are nearly the same for all three materials (path 0-1). However, the states of deformation at end of the isotropic loading phase differ quite noticeably (path 1-2). In particular, material type C predicted the largest deviatoric strain at end of the isotropic compression phase, which can be attributed to the assumed linear void ratio-logarithm of effective mean normal stress compressibility law. This deviatoric strain is predominantly plastic and arises from the normality condition even if the material is compressed isotropically from an initially anisotropic stress state.

Even though the compressibility laws are the same for material models A and B, the deviatoric strain at end of path 1-2 predicted by material type A is larger than that predicted by material type B by an amount equal to the elastic component produced by the elastic volumetric-deviatoric coupling inherent in material type B. The deviatoric strain differentials from isotropic loading (path 1-2) are carried over as the specimens deform further by deviatoric loading (path 2-3). As the specimens unload deviatorically (path 3-4), full recovery of elastic deviatoric strains is exhibited by material types A and B. Note in Fig. 8 that the slope of the unloading curve 3-4 for material type A is only about one-half of that for material type B, and that the unloading curve for material type C is nearly parallel to that for material type B.

The impact of the effective mean normal stress on the elastoplastic soil behavior is clearly demonstrated in this example. In contrast to the previous example of this section, where the effective mean normal stress remains nearly the same and therefore the three models predicted nearly the same behavior, the present example shows that significant variations in the predicted behavior could occur when the volumetric effective stress changes appreciably. Results of this study will have a significant impact on many geotechnical applications such as tunnelling and excavations, where elastic unloading, coupled by a reduction of the effective confining stress as well as plastic shear distortion, could dominate the structural response (Borja 1992).

Closed-Loop Elastic Loading

The objective of this section is to compare the elastic responses predicted by the same material models of the previous section to imposed closed stress path triaxial loading. This end can be pursued simply by prescribing an initial preconsolidation stress of p_{c0} = 360 kPa for all three material models and mimicking the second set of simulations of the previous section. A high value of p_{c0} causes all three specimens to remain overconsolidated throughout the duration of testing. Results of the numerical simulations are shown in Fig. 9.

Fig. 9(a) shows the material type A responses to imposed closed stress paths described in Table 2. Note that the model recovers completely all the elastic strains generated on the completion of the closed stress path. In particular, the volumetric strain-deviatoric strain curve of Fig. 9(a) shows that the volumetric and deviatoric responses are completely uncoupled. Fig. 9(b) also show a full recovery of elastic strains predicted by material type B, but two major differences are apparent: the sharp increase in the shear stiffness after the isotropic compression path 1-2, and the distorted shape of the response path produced by the volumetric-deviatoric elastic coupling [compare Figs. 9(a) and (b)].

Finally, Fig. 9(c) shows the responses predicted by material type C representing the hypoelastic model. Note that the total deviatoric strain is not fully recovered by the model after the completion of the closed stress path. This is to be expected since the elastic shear modulus is assumed to vary linearly with p, which in turn takes a constant value along the loading path 0-1 but a different constant value along the loading/unloading paths 2-3 and 3-4. Since the volumetric and deviatoric responses are not coupled, the elastic deformation is not fully recovered by the model. This example demonstrates that the hypoelastic model can exhibit a nonconservative elastic behavior even with a simple closed loading path.

SUMMARY AND CONCLUSIONS

A class of stored energy functions that includes the constant and variable elastic shear moduli cases is coupled with a critical-state plasticity model for clays. A bilogarithmic hardening law is used to describe the compressibility of the soil in the plastic regime. Stresses are integrated using a fully implicit numerical integration algorithm based on return mapping in the elastic strain invariant space.

Analyses of laboratory test results on a stiff overconsolidated Vallericca clay suggest that a variable shear modulus is more appropriate for this soil than a constant shear modulus elastic model. The shapes of the undrained stress paths observed in this clay just after load reversal indicate coupled volumetric and deviatoric elastic responses, a behavior that is captured naturally by the hyperelastic model. The pressure-dependent nature of the elastic shear modulus may have a noticeable effect, even in the plastic regime, when the value of the volumetric effective stress changes considerably. The proposed hyperelastic-plastic theory is capable of capturing this important effect, in addition to offering a fundamentally correct elastoplastic model that conserves elastic strain energy.

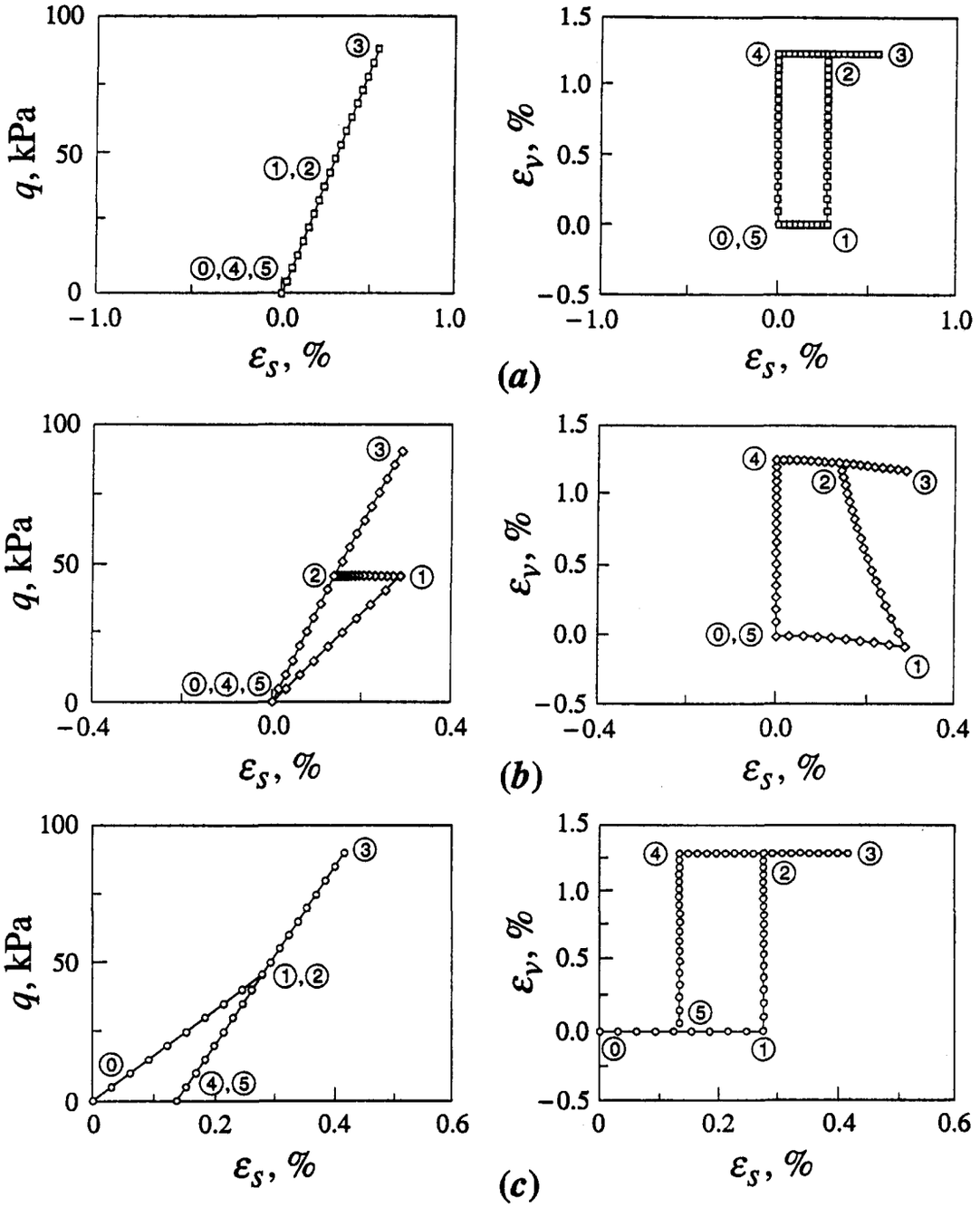

FIG. 9. Deviatoric Stress-Deviatoric Strain and Volumetric Strain-Deviatoric Strain Responses: (a) Material Type A; (b) Material Type B; (c) Material Type C

APPENDIX. REFERENCES

Alawaji, H., Runesson, K., and Sture, S. (1992). "Implicit integration in soil plasticity under mixed control for drained and undrained response." *Int. J. Numer. Anal. Methods in Geomech.*, 16, 737–756.

Amorosi, A. (1996). "Il comportamento meccanico di una argilla naturale consistente," PhD thesis, Università Degli Studi di Roma "La Sapienza," Rome, Italy.

Atkinson, J. H. (1981). *Foundations and slopes. An Introduction to applications of critical state soil mechanics.* John Wiley & Sons, Inc., New York, N.Y.

Borja, R. I. (1991). "Cam-clay plasticity, part II: Implicit integration of constitutive equation based on a nonlinear elastic stress predictor." *Comp. Methods Appl. Mech. Engrg.*, 88, 225–240.

Borja, R. I. (1992). "Free Boundary, fluid flow, and seepage forces in excavations." *J. Geotech. Engrg.*, ASCE, 118(1), 125–146.

Borja, R. I., and Alarcón, E. (1995). "A mathematical framework for finite strain elasto-plastic consolidation, part 1: Balance laws, variational formulation, and linearization." *Comp. Methods Appl. Mech. Engrg.*, 122, 145–171.

Borja, R. I., and Lee, S. R. (1990). "Cam-clay plasticity, part I: Implicit integration of elasto-plastic constitutive relations." *Comp. Methods Appl. Mech. Engrg.*, 78, 49–72.

Borja, R. I., and Tamagnini, C. (1995). "Finite deformation theory for a Cam-clay model." *Numerical models in geomechanics*, G. N. Pande and S. Pietruszczak, eds., NUMOG V, A. A. Balkema, Rotterdam, The Netherlands, 3–8.

Boyce, H. R. (1980). "A non-linear model for the elastic behaviour or granular materials under repeated loading." *Proc., Int. Symp. on Soils under Cyclic and Transient Loading*, 1, 285–294.

Britto, A. M., and Gunn, M. J. (1987). *Critical state soil mechanics via finite elements.* John Wiley & Sons, Inc., New York, N.Y.

Butterfield, R. (1979). "A natural compression law for soils." *Géotechnique*, London, England, 29, 469–480.

Dafalias, Y. F. (1986). "Bounding surface plasticity, I: Mathematical foundation and hypoplasticity." *J. Engrg. Mech.*, ASCE, 112(9), 966–987.

Dafalias, Y. F., and Herrmann, L. R. (1982). "Bounding surface formulation of soil plasticity." *Soil mechanics—transient and cyclic loads*, G. N. Pande and O. C. Zienkiewicz, eds., John Wiley & Sons, Inc., 253–282.

Duncan, J. M. (1996). "State of the art: Limit equilibrium and finite-element analysis of slopes." *J. Geotech. Engrg.*, ASCE, 122(7), 577–596.

Gens, A. (1982). "Stress-strain and strength characteristics of a low plasticity clay," PhD thesis, Univ. of London, London, England.

Gens, A., and Potts, D. M. (1988). "Critical state models in computational geomechanics." *Engrg. Computations*, 5, 178–197.

Hashash, Y. M. A., and Whittle, A. J. (1992). "Integration of the modified Cam-clay model in non-linear finite element analysis." *Comp. and Geotech.*, 14, 59–83.

Hashiguchi, K. (1995). "On the linear relations of V-ln p and ln v-ln p for isotropic consolidation of soils." *Int. J. Numer. Anal. Methods Geomech.*, 19, 367–376.

Hashiguchi, K., and Ueno, M. (1977). "Elasto-plastic constitutive laws of granular materials." *Constitutive equations of soils, Proc., Ninth Int. Conf. Soil Mech. Found. Engrg.*, Specialty Session 9, S. Murayama and A. N. Schofield, eds., 73–82.

Hill, R. (1967). *The mathematical theory of plasticity*. Oxford University Press, London, England.

Houlsby, G. T. (1985). "The use of a variable shear modulus in elastic-plastic models for clays." *Comp. and Geotech.*, 1, 3–13.

Hueckel, T., Tutumluer, E., and Pellegrini, R. (1992). "A note on non-linear elasticity of isotropic overconsolidated clays." *Int. J. Numer. Anal. Methods Geomech.*, 16(8), 603–618.

Hughes, T. J. R. (1984). "Numerical implementation of constitutive models: Rate independent deviatoric plasticity." *Theoretical foundations for large-scale computations of non-linear material behaviour*, S. Nemat-Nasser, R. Asaro, and G. Hegemier, eds., Martinus Nijhoff Publishers, Dordrecht, The Netherlands, 29–57.

Jaky, J. (1944). "The coefficient of earth pressure at rest." *Magyar Mérnök és Epitész Egglet Közlönye*, Budapest, Hungary, 355–358.

Jardine, R. J., Potts, D. M., Fourie, A. B., and Burland, J. B. (1986). "Studies of the influence of non-linear stress-strain characteristics in soil-structure interaction." *Géotechnique*, London, England, 36, 377–396.

Kachanov, L. M. (1971). *Foundations of the theory of plasticity*. North-Holland Publishing Co., Amsterdam, The Netherlands.

Lade, P. V., and Nelson, R. B. (1987). "Modelling the elastic behaviour of granular materials." *Int. J. Numer. Anal. Methods Geomech.*, 11, 521–542.

Loret, B. (1985). "On the choice of elastic parameters for sand." *Int. J. Numer. Anal. Methods Geomech.*, 9(3), 285–292.

Mayne, P. W., and Kulhawy, F. H. (1982). "K_0-OCR relationships in soils." *J. Geotech. Engrg. Div.*, ASCE, 108(6), 851–872.

Molenkamp, F. (1988). "A simple model for isotropic non-linear elasticity of frictional materials." *Int. J. Numer. Anal. Methods Geomech.*, 12(5), 467–475.

Mroz, Z., and Norris, V. A. (1982). "Elastoplastic and viscoplastic constitutive models for soils with application to cyclic loading." *Soil mechanics—transient and cyclic loads*, G. N. Pande and O. C. Zienkiewicz, eds., 173–217.

Ortiz, M., and Simo, J. C. (1986). "An analysis of a new class of integration algorithms for elastoplastic constitutive relations." *Int. J. Numer. Meth. Engrg.*, 23, 353–366.

Rampello, S., Viggiani, G., and Silvestri, F. (1994). "The dependence of small strain stiffness on stress state and history for fine grained soils: The example of Vallericca clay." *Pre-failure deformation of geomaterials*, Shibuya, Mitachi and Miura, eds., A. A. Balkema, Rotterdam, The Netherlands, 272–278.

Rampello, S., Viggiani, G., and Silvestri, F. (1995). "Panelist discussion: The dependence of G_0 on stress state and history." *Pre-failure deformation of geomaterials*, Shibuya, Mitachi and Miura, eds., A. A. Balkema, Rotterdam, The Netherlands, 1155–1160.

Roscoe, K. H., and Burland, J. H. (1968). "On the generalized stress-strain behavior of 'wet' clay." *Engineering plasticity*, J. Heyman and F. A. Leckie, eds., Cambridge University Press, London, England, 535–609.

Schofield, A., and Wroth, P. (1968). *Critical state soil mechanics*, McGraw-Hill Inc., New York, N.Y.

Simo, J. C. (1992). "Algorithms for static and dynamic multiplicative plasticity that preserve the classical return mapping schemes of the infinitesimal theory." *Comp. Methods Appl. Mech. Engrg.*, 99, 61–112.

Simo, J. C., and Meschke, G. (1993). "A new class of algorithms for classical plasticity extended to finite strains. Application to geomaterials." *Computational Mech.*, 11, 253–278.

Simpson, B. (1973). "Finite elements applied to problems of plane strain deformation in soil." PhD thesis, Univ. of Cambridge, Cambridge, England.

Vermeer, P. A. (1978). "A double hardening model for sand." *Géotechnique*, 28(4), 413–433.

Wroth, C. P. (1972). "Some aspects of the elastic behaviour of overconsolidated clay." *Proc., Roscoe Memorial Symp.: Stress-Strain Behaviour of Soils*, R. H. G. Parry, ed., G. T. Foulis and Co. Ltd., Oxfordshire, 347–361.

Wroth, C. P., and Houlsby, G. T. (1985). "Soil mechanics—property characterization and analysis procedure." *Proc., Eleventh Int. Conf. Soil Mech. Found. Engrg.*, A. A. Balkema, Rotterdam, The Netherlands, 1, 1–55.

Zytynski, M., Randolph, M. K., Nova, R., and Wroth, C. P. (1978). "On modeling the unloading-reloading behaviour of soils." *Int. J. Numer. Anal. Methods Geomech.*, 2, 87–93.